05 Oct 2015

Coalescence-Induced Jumping of Nanoscale Droplets on Super-Hydrophobic Surfaces

Zhi Liang
Missouri University of Science and Technology, zlch5@mst.edu

Pawel Keblinski

Recommended Citation

Z. Liang and P. Keblinski, "Coalescence-Induced Jumping of Nanoscale Droplets on Super-Hydrophobic Surfaces," *Applied Physics Letters*, vol. 107, no. 14, article no. 143105, American Institute of Physics, Oct 2015.
The definitive version is available at https://doi.org/10.1063/1.4932648

Applied Physics Letters

Coalescence-induced jumping of nanoscale droplets on super-hydrophobic surfaces

Cite as: Appl. Phys. Lett. **107**, 143105 (2015); https://doi.org/10.1063/1.4932648
Submitted: 03 August 2015 • Accepted: 26 September 2015 • Published Online: 06 October 2015

Zhi Liang and Pawel Keblinski

Coalescence-induced jumping of nanoscale droplets on super-hydrophobic surfaces

Zhi Liang[1,a)] and Pawel Keblinski[1,2,b)]
[1]*Rensselaer Nanotechnology Center, Rensselaer Polytechnic Institute, Troy, New York 12180, USA*
[2]*Department of Materials Science and Engineering, Rensselaer Polytechnic Institute, Troy, New York 12180, USA*

(Received 3 August 2015; accepted 26 September 2015; published online 6 October 2015)

The coalescence-induced jumping of tens of microns size droplets on super-hydrophobic surfaces has been observed in both experiments and simulations. However, whether the coalescence-induced jumping would occur for smaller, particularly nanoscale droplets, is an open question. Using molecular dynamics simulations, we demonstrate that in spite of the large internal viscous dissipation, coalescence of two nanoscale droplets on a super-hydrophobic surface can result in a jumping of the coalesced droplet from the surface with a speed of a few m/s. Similar to the coalescence-induced jumping of microscale droplets, we observe that the bridge between the coalescing nano-droplets expands and impacts the solid surface, which leads to an acceleration of the coalesced droplet by the pressure force from the solid surface. We observe that the jumping velocity decreases with the droplet size and its ratio to the inertial-capillary velocity is a constant of about 0.126, which is close to the minimum value of 0.111 predicted by continuum-level modeling of Enright *et al*. [ACS Nano **8**, 10352 (2014)]. © *2015 AIP Publishing LLC*.
[http://dx.doi.org/10.1063/1.4932648]

When two droplets coalesce on a super-hydrophobic surface, the released surface energy is partially converted to the kinetic energy of the coalesced droplet, which may lead to the jumping of the coalesced droplet from the surface. This interesting phenomenon has been recently reported in a variety of experiments and numerical simulations,[1–5] and has potential applications for heat pipes,[6] thermal diodes,[7] self-cleaning surfaces,[8] and energy harvesting.[9]

Generally, a droplet has a nearly-spherical shape on a super-hydrophobic surface if its size is far smaller than the capillary length. For two equally sized spherical droplets coalescing on a super-hydrophobic surface, numerous experimental and modeling results[1,2,4,5,10] show that the jumping velocity, v_j, of a coalesced droplet increases with decreasing droplet size and roughly follows the inertial-capillary scaling (where viscous dissipation is negligible)[1] $v_j \propto U = \sqrt{\gamma_{lv}/\rho R}$ where U, γ_{lv}, ρ, and R are the inertial-capillary velocity, liquid-vapor surface tension, density, and initial radii of the droplets, respectively. When R is smaller than $\sim$50 μm, however, some studies[1,2,5,10] show that v_j no longer follows the inertial-capillary scaling and begins to decrease rapidly with decreasing R. This is attributed to viscous dissipation leading to no observable jumping below R of $\sim$10 μm.

The recent experimental and modeling work by Enright *et al*.,[4] however, found that v_j continuously increases with decreasing R even when R is reduced to $\sim$5 μm. They attributed the observation of no jumping of small droplets in the previous studies to the influence of surface adhesion in previous experiments and a neglect of the details of the evolving droplet morphology in energy-based modeling.[4] The smallest droplet size studied in the work of Enright *et al*. is $R \approx 5$ μm, where the highest v_j is achieved. This raises a question of whether the increase of v_j will continue if R is further reduced to submicron size.

The experimental study of dynamics of submicro-sized droplets is currently very challenging, partially due to the limited time resolution of microscopic image capturing systems in the experiment.[4,11] In this work, we resorted to molecular dynamics (MD) simulations to investigate the coalescence of nanoscale droplets on a super-hydrophobic surface. With such approach, we were able to simulate coalescence of droplets with sizes up to 50 nm, without any assumption underlying continuum-level modeling.

The model systems consist of solid Au in contact with liquid Ar droplets at a temperature of 85 K, as depicted in Fig. 1. The Au slab is placed at the bottom of the simulation box, and periodic boundary conditions (PBCs) are applied in all three directions. The Au slab is formed by three (111) oriented Au atomic layers. The atoms in the center layer are kept fixed during the simulations.

The embedded-atom-method (EAM) potential[12] is used for Au-Au interactions. The Ar-Ar interaction and Ar-Au interaction are of the Lennard-Jones type

$$V_{ij} = 4\varepsilon[(\sigma/r)^{12} - c_{ij}(\sigma/r)^6], \tag{1}$$

with parameters $\sigma = 3.41$ Å and $\varepsilon = 10.3$ meV.[13] The coefficient c_{ij} is equal to 1 for the Ar-Ar interaction, and is tuned to low values for the Ar-Au interaction to adjust the droplet contact angle and the adhesion energy on the solid surface and thus to mimic a super-hydrophobic surface. To save the computational time, we set the cutoff distance $r_{cut} = 2.5\sigma$. The velocity Verlet algorithm with a time step size of 6 fs is used to integrate the equations of motions in all MD simulations.[14]

For the analysis of the coalescence dynamics, using equilibrium MD simulations, we determined the saturation pressure, liquid-vapor surface tension, density, and viscosity

a)Electronic mail: liangz3@rpi.edu.
b)Electronic mail: keblip@rpi.edu.

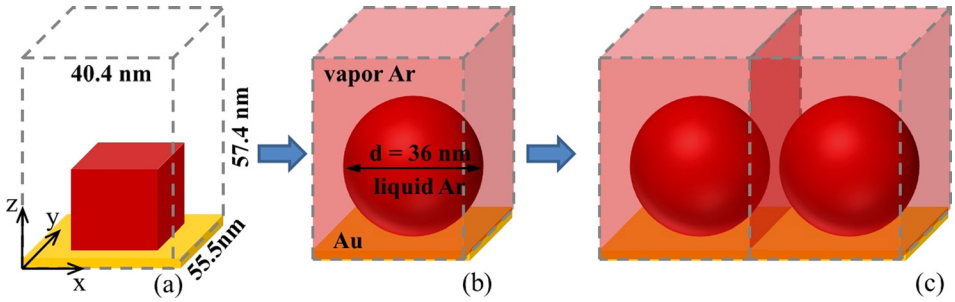

FIG. 1. Schematic diagram of the procedure for the generation of two 36-nm droplets on a super-hydrophobic surface. (a) A cubic Ar crystal on Au surface. (b) A 36-nm Ar droplet on a super-hydrophobic surface. (c) Two identical droplets on the Au surface created by the duplication of simulation box in the x-direction.

of the model fluid Ar with $r_{cut} = 2.5\sigma$ at 85 K. We note that this cutoff of 2.5σ, while routinely used in modeling of bulk fluids, leads to significant under-prediction of the surface tension (increasing the cutoff to 4σ results in 50% increase of the surface tension) and viscosity, and over-prediction of the saturated pressure. Our goal, however, is not to study argon fluid specifically, but the nanodroplet jumping in general, and, for this purpose, the cutoff of 2.5σ is simply a part of the model fluid definition.

The simulation detail is described in our previous work.[15,16] Briefly, we placed a liquid slab of 2160 Ar atoms in the middle of a simulation box which has a length of 19.2 nm and cross section area of 3.84 nm by 3.84 nm. The box size is fixed during the simulation, and PBCs are applied in all three directions. We equilibrated the system at 85 K using the Berendsen thermostat.[17] After the system reaches thermal equilibrium, a liquid and vapor phase separated by two planar liquid-vapor interfaces was present in the same simulation cell. We then monitor the value of the pressure tensor in 200 planar bins. The surface tension is obtained by using the mechanical definition according to Irving and Kirkwood.[18,19] The saturation pressure, P_{sat}, is the average value of pressure normal to the liquid-vapor interface. From the simulation, we found $\gamma_{lv} = 8.16 \pm 0.04$ mJ/m^2 and $P_{sat} = 2.15$ atm.

To evaluate the viscosity, η, and density, ρ, of the saturated liquid Ar, we first placed a bulk liquid Ar of 4000 atoms in a cubic simulation box with PBCs applied in three directions and equilibrated the bulk liquid to 85 K and 2.15 atm using the algorithm of Berendsen *et al.*[17] After the system reached the desired temperature and pressure, we turned off the thermostat and barostat and carried out the simulation in the microcanonical ensemble to determine viscosity from the running integral of the shear-stress correlation function.[20,21] Using the above described procedure, we found $\rho_{liquid} = 1.31 \times 10^3$ kg/m^3, $\eta_{liquid} = 190 \pm 1$ μPa·s.

Now, we turned our attention to MD simulations of coalescence of nanoscale droplets on a super-hydrophobic surface. To create a stable Ar droplet on an Au surface, we first placed a [100]-orientated perfect FCC crystal Ar with the lattice constant of 5.4 Å on the Au surface. The crystal Ar contains 50 unit cells in each of the x, y, and z directions. The dimension of the simulation box is 40.4 nm × 55.5 nm × 57.4 nm as shown in Fig. 1(a). The box size is fixed during the simulation.

After initialization, the fluid Ar and the solid Au were equilibrated separately with the Berendsen thermostat[17] to a temperature of 85 K. To avoid the departure of droplet from the surface during the equilibration, the Ar-Au interaction coefficient c_{ij} in Eq. (1) was first set to 0.3 to provide enough surface adhesion. As the system is equilibrated to 85 K, the crystal Ar melted and partially vaporized to establish a liquid-vapor coexisting phase in the simulation box. After 4 ns, a stable liquid droplet formed on the Au substrate. Subsequently, we gradually tuned the Ar-Au interaction coefficient down to 0.2 and equilibrated the system for another 6 ns. Finally, we turned off the thermostat in the fluid and equilibrated the system for another 4 ns to damp out the oscillations in the droplet. By this method, we obtained a stable droplet on a super-hydrophobic surface with a diameter of ~36 nm and a contact angle approaching 180°, as depicted in Fig. 1(b).

The equilibrated structure is then duplicated in the x direction to create two identical liquid droplets on the Au substrate as shown in Fig. 1(c). The total number of atoms in the liquid phase is about 1 000 000. To make the two droplets coalesce, we assigned the x-direction velocity, v_x, of +/− 3 m/s to Ar atoms in the left/right half of the simulation box and carried out MD simulations for 7 ns. The thermostat is applied to the solid substrate in all the simulations. To distinguish the liquid and vapor phases in the simulation, we define an Ar atom as liquid if its potential energy is lower than half of that in a saturated bulk liquid at 85 K. With this definition, the z-component velocity, v_z, of liquid droplets as a function of time is calculated and shown in Fig. 2(a). The Au slab has two surfaces. We define the one in direct contact with the droplets as the bottom surface and the other in contact with the vapor phase on the top the simulation box through PBCs as the top surface. The average pressure on the two surfaces (P_{top} and P_{bottom}) as a function of time is shown in Fig. 2(b). Additionally, we show temporal evolution of the solid and fluid temperatures in Fig. 2(c).

The results in Fig. 2 indicate that the simulated coalescence process can be divided into five stages. Stage I (0 ns ~ 0.6 ns): The two droplets approach each other, and the coalescence has not started. At this stage, v_z is essentially a constant around 0.1 m/s. The small nonzero v_z mainly comes from the thermal motions of the two droplets. As the size of droplets gets larger, the v_z at this stage will be even smaller. P_{top} and P_{bottom} are both around 2.3 atm which is higher than $P_{sat} = 2.15$ atm. The slightly increased vapor pressure is associated with the large curvature of the liquid-vapor interface.[22] The solid and fluid temperatures both fluctuate around 85 K at this stage.

Stage II (0.6 ns ~ 1.6 ns): The two droplets touch each other (see the snapshot I|II in Fig. 2(d)), and coalescence starts. The surface pressure is essentially the same as that in Stage I. The fluid temperature starts to increase due to the

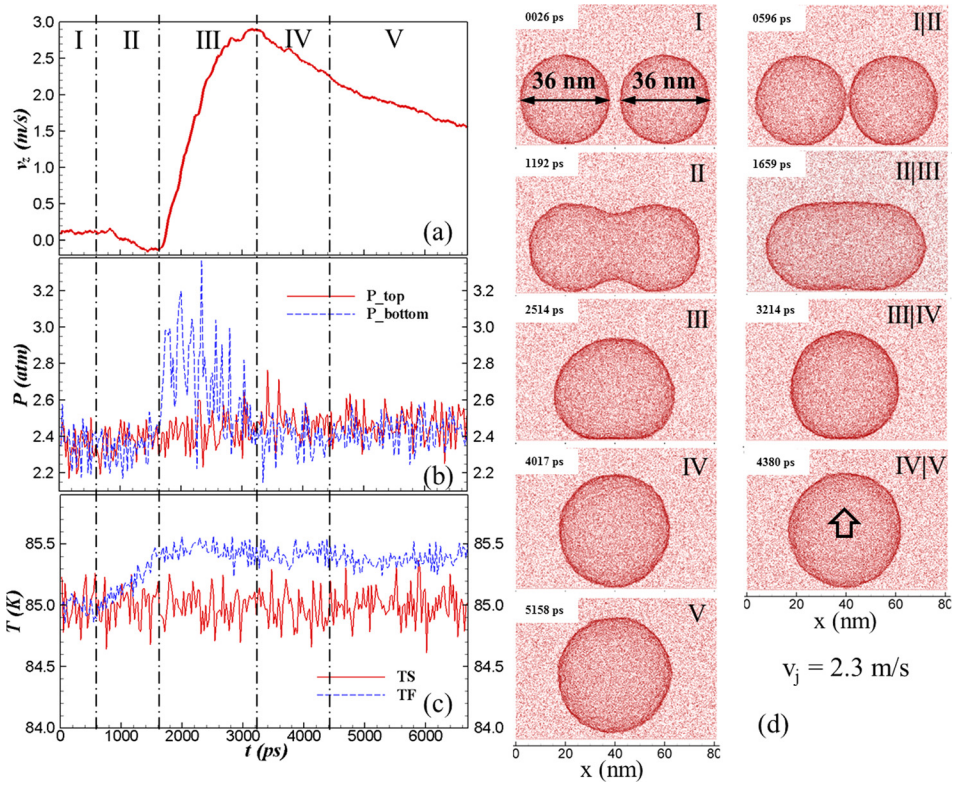

FIG. 2. The temporal evolution of (a) velocity of droplets in the z-direction; (b) average pressure on the bottom and top surfaces of the Au slab; (c) temperature of Au slab (TS) and temperature of fluid (TF) during the coalescence of two droplets. (d) Snapshots of droplet coalescence on a super-hydrophobic surface. The first column in (d) is a typical snapshot in each of the five stages. The second column is the snapshot at the moment of transition from one stage to another.

conversion of excess surface energy into thermal and kinetic energy of droplets.

At this stage, a bridge between droplets forms and expands rapidly. In the inertial regime, the bridge width r_b evolves with time t as $r_b/R = C_b\sqrt{t/\tau}$, where $\tau = \sqrt{\rho_{liquid}R^3/\gamma_{lv}}$ is the inertial-based time scale of the coalescence process and C_b is a constant of the order of unity.[11,23] This scaling is valid when r_b is greater than the viscous length $l_v = \eta^2_{liquid}/\rho_{liquid}\gamma_{lv}$. With the fluid properties found in the earlier MD simulations, we obtained $l_v \approx 3.38$ nm. Since the droplet size in the simulation is much larger than this value, the evolution of the coalescence bridge is essentially in the inertial regime except at the very early times of the coalescence when r_b is very small. This is indeed the case as demonstrated in Fig. 3 showing a linear relationship between r_b/R and $\sqrt{t/\tau}$ with a slope of 0.90. At this stage, v_z varies between ± 0.1 m/s, which is again mainly caused by the thermal motions of droplets.

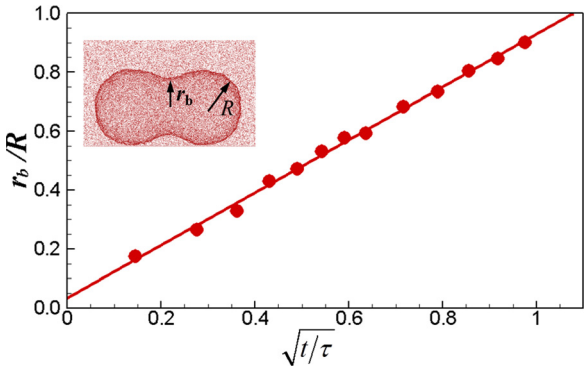

FIG. 3. The ratio of bridge width (r_b) to radius of the droplets ($R = 18$ nm) as a function of $\sqrt{t/\tau}$, where t is the time measured from the moment at which the two droplets just touch each other. The straight line is the linear fit to the simulation data points and the slope of the straight line is 0.90.

Stage III (1.6 ns ~ 3.2 ns): The expanding bridge impacts the solid surface (see the snapshot II|III in Fig. 2(d)), which leads to acceleration of the coalesced droplet by the pressure force from the solid surface. At this stage, high pressure builds up at the bottom of the coalesced droplet. As a result, P_{bottom} is evidently higher than P_{top} (see Fig. 2(b)). The high P_{bottom} accelerates the coalesced droplet in the z direction, which results in an upward momentum large enough to lift the droplet away from the surface. At the end of this stage, the coalesced droplet has a nearly-spherical shape (see snapshot III|IV in Fig. 2(d)), the value of P_{bottom} drops to that of P_{top}, and acceleration stops.

A similar acceleration process was also observed in previous continuum-level simulations of coalescence-induced jumping of microscale droplets.[3–5] This finding suggests that the mechanism of coalescence-induced jumping of nanoscale droplets is the same as that of microscale droplets. However, our MD simulation results are not consistent with the recent phase-field simulation results,[5] which show that the liquid bridge no longer impacts the solid surface as the droplet size is reduced from microscale to nanoscale. The inconsistency might be caused by the no-slip boundary condition imposed in the phase-field simulation,[5] since the slip length of fluid on a super-hydrophobic surface could reach tens of nanometers, which is non-negligible for nanoscale systems.[16,24] In fact, for our model system, we estimated the slip length to be about 90 nm.[16]

Stage IV (3.2 ns ~ 4.4 ns): The coalesced droplet starts to detach from the solid surface. At this stage, the droplet continues to move up. However, the bottom of the droplet is still in contact with the solid surface (see snapshot IV in Fig. 2(d)). This results in the deceleration of the droplet as shown

in Fig. 2(a) and slightly lower P_{bottom} than P_{top} as shown in Fig. 2(b). At the end of this stage, the coalesced droplet completely detaches from the solid surface with the speed of $v_j = 2.29 \pm 0.11$ m/s (see snapshot IV|V in Fig. 2(d)). The uncertainty of v_j is determined from three independent runs.

Stage V (> 4.4 ns): The departed droplet moves up in vapor, and no discernable oscillations of droplet were observed due to the significant viscous dissipation in the nano-droplet. The deceleration of droplet at this stage is caused by the Stokes drag from the vapor. As shown in Fig. 2(b), the P_{bottom} and P_{top} in this stage are higher than those in Stage I. The higher pressure at this stage is caused by the enhanced temperature in the fluid system as shown in Fig. 2(c).

To ensure that the coalescence-induced jumping found in the above simulation is not affected by the initial v_x assigned to the fluid, we reduced the v_x from ±3 m/s to ±1.5 m/s and ±0.5 m/s. The resulting v_j varies between 2.18 m/s and 2.30 m/s, which indicates that v_j is essentially independent of initial v_x in the range of v_x simulated. To save the computational cost, therefore, we assign the initial $v_x = \pm 3$ m/s to the fluid in all the subsequent simulations.

With a jumping velocity of $v_j = 2.29$ m/s, we determine that the kinetic energy of the center of mass of the droplet, E_j, is only ~1.3% of the available excess surface energy, $\Delta E_S = 4\pi\gamma_{lv}R^2(2 - 2^{2/3})$. For $R = 18$ nm, the Ohnesorge number, $Oh = \eta_{liquid}/\sqrt{\rho_{liquid}\gamma_{lv}R}$, of the coalescence process is 0.44. As a comparison, the lowest energy conversion efficiency, $E_j/\Delta E_S$, for the coalescence of microscale droplets in the study of Enright *et al.*[4] is 1.8% for $Oh = 0.12$. The decrease of energy conversion efficiency with an increasing Oh number was observed in experimental and numerical study of microsized droplets in Enright *et al.*[4] As the Oh number in our model is much greater, a more pronounced viscous dissipation and a lower energy conversion efficiency found in nano-droplets coalescence are reasonable.

To study the size effect on coalescence and jumping of nanoscale droplets, we varied the diameter of the droplets in the MD simulation from 22.7 nm to 53.3 nm, which corresponds to the Oh number variation from 0.36 to 0.55. The simulation results show that the coalescence-induced droplet jumping processes for the five simulated droplet sizes are all similar and the jumping velocity follows the inertial-capillary scaling law, $v_j \propto U = \sqrt{\gamma_{lv}/\rho R}$, as shown in Fig. 4. When v_j is scaled by the inertial-capillary velocity U, the dimensionless jumping velocity, v_j/U, is a constant around 0.126 over the range of Oh simulated. This also indicates that energy conversion efficiency, $E_j/\Delta E_S$, is essentially the same for all the simulated droplet sizes. For reference, we included in Fig. 4, the relationship between v_j/U and Oh obtained in the study of Enright *et al.*,[4] where v_j/U was determined from finite-element-based simulations of micro-droplet coalescence process. Enright *et al.* show that their numerical predictions agree very well with their experimental data and a quadratic fit to their numerical data predicts the minimum v_j/U value of 0.111,[4] which is close to $v_j/U = 0.126$ in our MD simulations.

In summary, we used MD simulations to study coalescence of two equal sized nanoscale droplets on a super-hydrophobic surface. Although about 99% of the available excess surface energy is dissipated by the internal viscous force during the coalescence process, the jumping velocity of nanoscale droplets in this study can still reach a relatively high value of 2–3 m/s due to the very large surface-to-volume ratio of nanoscale droplets. The simulation results show that the external force that pushes the droplet away from the surface was exerted by the solid surface, which is impacted by the expanding liquid bridge between the two coalescing droplets. Over the range of Oh simulated ($Oh = 0.36 - 0.55$), we found that the jumping velocity of coalesced droplet follows the inertial-capillary scaling law, and the dimensionless jumping velocity equals 0.126, which is close to the minimum value of 0.111 predicted by finite-element-based simulations.

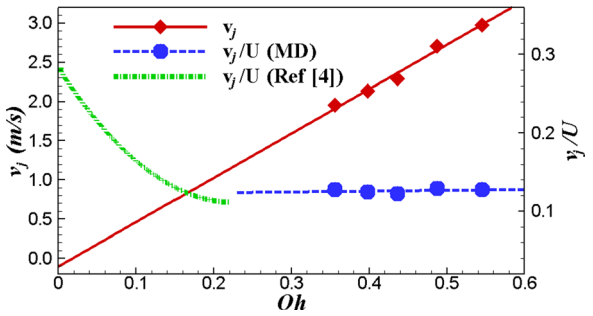

FIG. 4. The jumping velocity (v_j) and dimensionless jumping velocity (v_j/U) of the merged droplet as a function of Oh number. The red solid line is the linear fit to v_j vs. Oh. The blue dashed line is the linear fit to v_j/U vs. Oh. The green dashed-dotted line is from Ref. 4, in which the finite-element-based method is used to determine the jumping velocity of microscale water droplets on a surface with no adhesion.

This work was supported by the U.S. Air Force Office of Scientific Research Grant No. FA9550-12-1-0351. We would like to thank Professor Yunfeng Shi and Professor Joel Koplik for useful discussions on this project, and thank eXtreme Science and Engineering Discovery Environment (XSEDE) for providing us supercomputer resources for MD simulations.

[1]J. B. Boreyko and C. Chen, Phys. Rev. Lett. **103**, 184501 (2009).
[2]C. Lv, P. Hao, Z. Yao, Y. Song, X. Zhang, and F. He, Appl. Phys. Lett. **103**, 021601 (2013).
[3]Y. S. Nam, H. Kim, and S. Shin, Appl. Phys. Lett. **103**, 161601 (2013).
[4]R. Enright, N. Miljkovic, J. Sprittles, K. Nolan, R. Mitchell, and E. N. Wang, ACS Nano **8**, 10352 (2014).
[5]F. Liu, G. Ghigliotti, J. J. Feng, and C. Chen, J. Fluid Mech. **752**, 39 (2014).
[6]N. Miljkovic, R. Enright, Y. Nam, K. Lopez, N. Dou, J. Sack, and E. N. Wang, Nano Lett. **13**, 179 (2013).
[7]J. B. Boreyko, Y. Zhao, and C. Chen, Appl. Phys. Lett. **99**, 234105 (2011).
[8]K. M. Wisdom, J. A. Watson, X. Qu, F. Liu, G. S. Watson, and C. Chen, Proc. Natl. Acad. Sci. **110**, 7992 (2013).
[9]N. Miljkovic, D. J. Peterson, R. Enright, and E. N. Wang, App. Phys. Lett. **105**, 013111 (2014).
[10]F. Wang, F. Yang, and Y. Zhao, Appl. Phys. Lett. **98**, 053112 (2011).
[11]J.-C. Pothier and L. J. Lewis, Phys. Rev. B **85**, 115447 (2012).
[12]S. M. Foiles, M. I. Baskes, and M. S. Daw, Phys. Rev. B **33**, 7983 (1986).
[13]G. C. Maitland, M. Rigby, E. B. Smith, and W. A. Wakeham, *Intermolecular Forces: Their Origin and Determination* (Clarendon Press, Oxford, 1981).
[14]D. Frenkel and B. Smit, *Understanding Molecular Simulation* (Academic Press, San Diego, 2002), p. 75.
[15]Z. Liang, K. Sasikumar, and P. Keblinski, Phys. Rev. Lett. **111**, 225701 (2013).

[16]Z. Liang and P. Keblinski, J. Chem. Phys. **142**, 134701 (2015).
[17]H. J. C. Berendsen, J. P. M. Postma, W. F. Van Gunsteren, A. Di Nola, and J. R. Haak, J. Chem. Phys. **81**, 3684 (1984).
[18]J. P. R. B. Walton, D. J. Tildesley, J. S. Rowlinson, and J. R. Henderson, Mol. Phys. **48**, 1357 (1983).
[19]J. G. Kirkwood and F. P. Buff, J. Chem. Phys. **17**, 338 (1949).
[20]Z. Liang and H.-L. Tsai, Fluid Phase Equilibria **293**, 196 (2010).
[21]Z. Liang and H.-L. Tsai, Mol. Phys. **108**, 1285 (2010).
[22]R. J. Hunter, *Foundations of Colloid Science*, 2nd ed. (Oxford University Press, 2001).
[23]J. Eggers, J. R. Lister, and H. A. Stone, J. Fluid Mech. **401**, 293 (1999).
[24]J.-L. Barrat and L. Bocquet, Phys. Rev. Lett. **82**, 4671 (1999).